

# HIGH-STRENGTH STEELS IN WELDED STATE FOR LIGHT-WEIGHT CONSTRUCTIONS UNDER HIGH AND VARIABLE STRESS PEAKS

Heinz Kaufmann - Fraunhofer Institute for Structural Durability and System Reliability LBF  
Cetin Morris Sonsino - Fraunhofer Institute for Structural Durability and System Reliability LBF  
Guisepe Demofonti - Centro Sviluppo Materiali CSM  
Sandro Riscifuli - Centro Sviluppo Materiali CSM

## ABSTRACT

In design codes (Eurocode, British Standard and others) for the dimensioning of welded joints, no distinction is made between low-, medium- and high-strength steels. Because of a lack of general knowledge about the benefits of high-strength steels and also because of missing information in design codes, in many cases design engineers still use low- or medium-strength steels ( $R_{p0.2} < 400$  MPa) and compensate for high loads under constant or variable amplitude loading or overloads by increasing dimensions. Given this situation, it was deemed necessary to establish criteria for the design of light-weight welded constructions under high and variable stress peaks using new classes of high-strength steels, such as S355N (normalized), S355M (thermomechanically treated), S690Q (water quenched) and S960Q (water quenched), and to perform more reliable evaluations of the fatigue performance of high-strength steel structures subjected to complex loading with regard to light-weight design and economics. For the comparison of the fatigue strengths of the investigated steels the notch factors present were taken into account. Additionally, the real damage sums were determined in order to give recommendations for the fatigue life estimation, i.e.  $D_{al} = 0.5$ .

Under constant amplitude loading, no significant difference in the bearable local stress amplitudes for the butt welds can be detected for the four investigated steels. Under variable amplitude loading, the butt welded (lower notch factor) high strength steel S960Q has advantages in the case of the normal Gaussian spectrum and in the case of overloads, especially under pulsating loading. For the transverse stiffeners (high notch factor), slight advantages for the high strength steel S960Q exist, only in the case of pulsating overloads. However, the advantages of high strength steels in case of static loading are indisputable. In most of the investigated cases, overloads lead to a benefit in fatigue life.

## KEYWORDS

High-strength steels, butt weld, transverse stiffener, notch factor, Woehler and Gassner lines, stress ratio, overloads, fatigue life estimation.

## INTRODUCTION

The situation, that in design codes [1, 2, 3, 4] for the dimensioning of welded joints, no distinction between low-, medium- and high-strength steels is made, cannot be generalised for all types of loading. Because of the higher yield strength of high-strength steels, these steels should have advantages in light-weight design compared to low-strength steels when a variable amplitude loading, with high stress levels (cranes, bridges, offshore- and ship-structures) or special events, occurs. Because the expected advantages in relation to practically occurring loading types could not be demonstrated convincingly, design engineers have been conservative in the use of high-strength steels [5], which enable economical light-weight constructions.

# 1. MATERIALS, SPECIMEN GEOMETRIES AND LOADING

The mechanical properties for the steel grades investigated Fe E 355 (normalized, S355N, and thermomechanically treated, S355 M), Fe E 690 (waterquenched, S690Q), Fe E 960 (waterquenched, S960Q) are given in **Tab. 1**.

Materials	Position of specimen and rolling direction	Yield Strength $R_{p0.2\%}$ [MPa]	Tensile Strength $R_m$ [MPa]	Elongation ( $l_0/d = 5$ ) A [%]	Reduction of area Z [%]
S355N normalized	longitudinal	374	559	36	75
	transverse	378	560	36	77
S355M thermomechan. treated	transverse	422	524	33.5	-
S690Q waterquenched	longitudinal	786	870	22	73
	transverse	784	868	21	74
S960Q waterquenched	transverse	998	1072	15,5	-

**Tab. 1** Mechanical properties

This investigation was carried out with two types of joint, a butt joint and a cruciform joint with thickness of 30 mm. **Fig. 1** shows the dimensions of the specimens. The orientation of the weld position was perpendicular to the rolling direction. The specimens were cut from large welded plates ( $l = 1250$  mm). The weld toes at the edges of the specimens were locally ground to increase the fatigue life in these areas and therefore prevent cracks from forming at the outer edges. Weld preparation was required for the plates and was done by flame cutting. Data on the welding procedures with respect to particular steel qualities and thickness were already known by the steel makers and were applied for the production of the specimens (i.e. submerged arc welding, shielded arc welding, type of wire, intensity of current, symmetric welding,  $t_{8/5}$  (cooling time from  $t = 800$  °C to  $500$  °C)). Furthermore, the welding conditions were fixed after preliminary tests. Straightening of the specimens or plates after welding was not permitted. The welds in the test specimens fulfilled the requirements of the quality level "stringent" (B) according to ISO 5817 [6, 7]. The steel makers prepared the required profiles. All welds were required to be fully penetrated. In the case of the

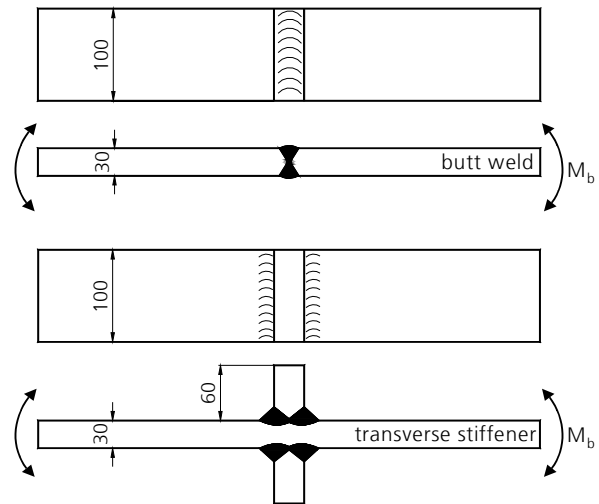


**Fig. 1** Dimension of the specimens (length  $l = 500$  mm)

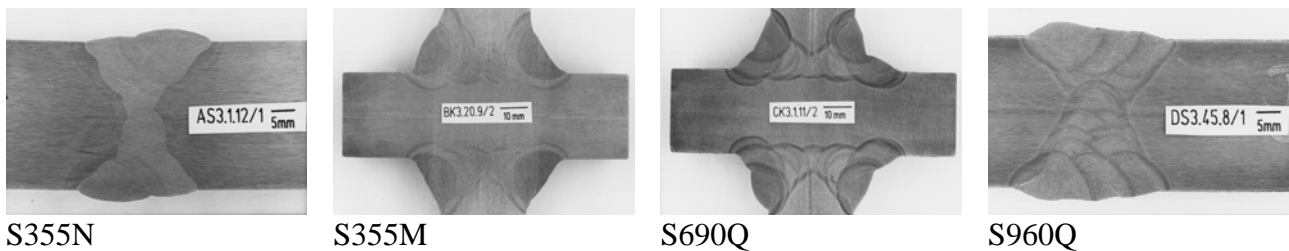


**Fig. 2** Shape of the welds

cruciform joint, a double HV-weld without convexity had to be welded. Moreover, these welds were carried out with a support bead. After welding, the weld quality was examined. Examples of the shape of the welded joints are displayed in **Fig. 2**. The specimens were investigated under 4-point-bending. The tests were carried out under constant amplitude and under variable amplitude loading with a base Gaussian spectrum as well as with the superimposing of a Gaussian overload spectrum to the normal Gaussian spectrum under fully reversed ( $R = -1$ ) or under pulsating ( $R = 0$ ) loading, **Fig. 3**. (This particular load type was based on the experience of crane manufacturers.) In

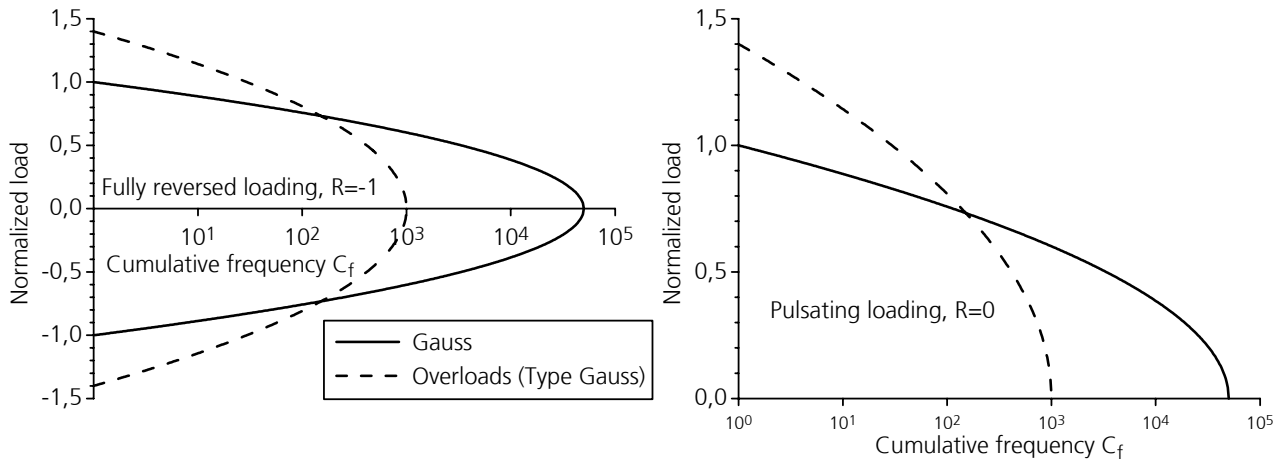


**Fig. 3** Load sequences and overloads

the case of the Gaussian spectrum, the sequence length is  $L_{s,G} = 5 \cdot 10^4$ ; in the case of the overloads  $L_{s,OL} = 10^3$ . The overloads are distributed randomly into the basic sequence and the total length of the total spectrum is also  $5 \cdot 10^4$  cycles. This is achieved by omitting the large amplitudes of the basic Gaussian spectrum at the point of intersection with the spectrum with overloads and the addition of the large amplitudes.

## 2. HARDNESS MEASUREMENTS

These measurements were carried out 2 mm below the surface of the sheets, **Tab. 2**.

Materials	Hardness HV1					
	base material		peaks in the HAZ		weld material	
	min.	max.	min.	max.	min.	max.
S355N normalized	160	170	280	290	220	250
S355M thermomechan. treated	160	180	220	240	200	240
S690Q waterquenched	280	300	430	480	300	370
S960Q waterquenched	360	380	400	450	360	420

**Tab. 2** Hardness values

S355N: The hardness in the weld metal is higher than in the base material. The highest hardness (peaks) occurs in the heat affected zone.

S355M: The hardness increases slightly from the base material, over the heat affected zone, to the weld metal.

S690Q: The hardness in the weld metal is a little higher than in the base material. There are peaks in the heat affected zone much higher than the hardness of the weld metal.

S960Q: The hardness in the weld metal is a little higher than in the base material. In the heat affected zone, peaks could be measured that were a little higher than in the weld metal.

### 3. NOTCH FACTORS

For each material, weld type and thickness (8 variants) the geometry (radius and angle) was measured in order to calculate the notch factor [8]. Many measurements and calculations were carried out and evaluated with statistical methods. **Fig. 4** demonstrates an example of the applied

10 % probability of occurrence	S355N	S355M	S690Q	S960Q
Butt welds	2.82	3.13	2.67	3.02
Transverse stiffeners	5.20	6.03	4.24	6.20

**Tab. 3** Statistical evaluation of the notch factors  $K_t$

Butt welds	S355N	S355M	S690Q	S960Q
Notch factor	2.93	2.65	2.56	2.76
probability of occurrence	6.9 %	32 %	16 %	20 %

**Tab. 4** Post mortem evaluation of the notch factors  $K_t$  in the crack initiation areas

procedure. In **Tab. 3** the statistical evaluation of the notch factors for all investigated geometries is presented. For both weld types, the geometries produced by the two steel manufacturers are significantly different. To calculate the local stresses, the highest notch factor (probability of occurrence of 10 %) will be used, because this value (or a higher one) will occur at each specimen and will be responsible for crack initiation. Spot check investigations were carried out at the location of crack initiation with tested butt welds, **Tab. 4**.

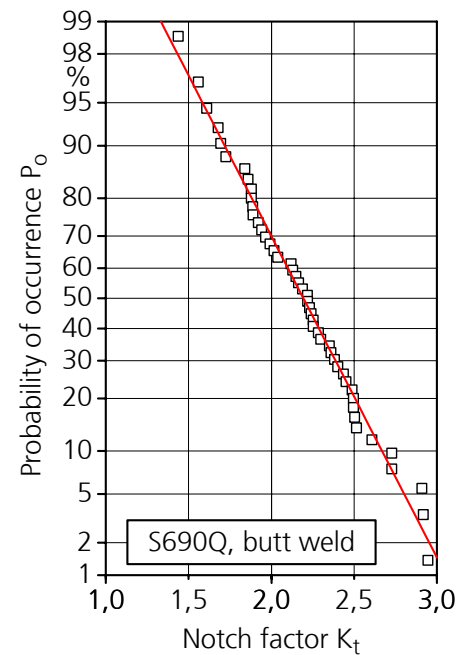


**Fig. 4** Notch factors

### 4. FATIGUE RESULTS FOR THE WELDED JOINTS

Based on the observation that features like the slope of the S-N curve, the position of the knee point and scattering are repeated in similar way, the concept of uniform scatter bands was used to analyse the S-N curves based on nominal stresses [9, 10]. This concept allows the course of the S-N curve to be fixed with few results if the same specimen geometry, similar material, surface condition and the same loading mode is assumed. But it is not always necessary to consider all features. The failure criterion was the cycles to rupture  $N_r$  respectively  $\bar{N}_r$ . The location of crack initiation was in all cases the transition from the weld metal into the heat affected zone (HAZ).

For constant amplitude loading, the knee point was fixed at  $N_e = 2 \cdot 10^6$  load cycles. For variable amplitude loading, the endurable stresses were assigned also to the reference load cycles  $\bar{N} = 2 \cdot 10^6$ . The butt welds have a slope of  $k = \bar{k} = 3.5$ , the transverse stiffeners  $k = \bar{k} = 3.25$ . Under constant amplitude loading after the knee point, a decrease of the S-N curve of 10 % ( $k = 22$ ) per decade was evaluated to consider possible failures in this region.

For the whole S-N curve a constant scatter band was assumed:

$$T_{\sigma} = 1 : \sigma_a(P_s=10\%) / \sigma_a(P_s=90\%) = 1 : 1.35 \quad (1)$$

This scatter band was also assumed for the tests under variable amplitude loading.

**Fig. 5** shows examples of the fatigue life results as Woehler (S-N) and Gassner lines. All results are presented in **Tab. 5** in the nominal stress system. Under constant amplitude loading, only negligible differences between the fatigue lives under fully reversed ( $R = -1$ ) and pulsating ( $R = 0$ ) loading are apparent. This indicates the existence of high tensile mean stresses.

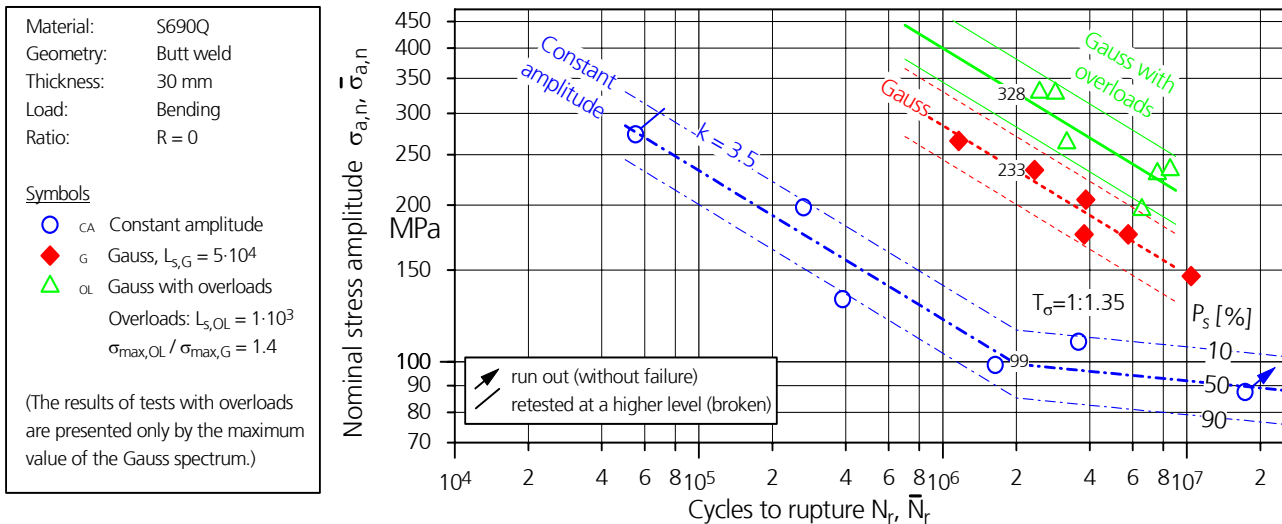


**Fig. 5** Fatigue test results

Materials	S-N curves (constant amplitudes)				Spectrum loading (Gauss)				Spectrum loading with special events (Gauss with overloads)			
	butt welds		transverse stiffeners		butt welds		transverse stiffeners		butt welds		transverse stiffeners	
	R=-1	R=0	R=-1	R=0	$\bar{R}=-1$	$\bar{R}=-1$	$\bar{R}=-1$	$\bar{R}=-1$	$\bar{R}=-1$	$\bar{R}=-1$	$\bar{R}=-1$	$\bar{R}=-1$
S355N	A: 99 B: 3.5	- -	- -	72 3.25	- -	- -	- -	- -	213 3.5	# #	187 3.25	# #
S355M	A: 77 B: 3.5	75 3.5	65 3.25	62 3.25	212 3.5	226 3.5	175 3.25	189 3.25	192 3.5	# #	171 3.25	# #
S690Q	A: 102 B: 3.5	99 3.5	90 3.25	90 3.25	220 3.5	233 3.5	236 3.25	267 3.25	221 3.5	328 3.5	268 3.25	274 3.25
S960Q	A: 83 B: 3.5	102 3.5	65 3.25	56 3.25	263 3.5	305 3.5	189 3.25	182 3.25	275 3.5	410 3.5	155 3.25	231 3.25

A: Fatigue Data  $\sigma_{a,e}$  respectively  $\bar{\sigma}_a$  in MPa (nominal stresses) at the knee points  $N_e$  respectively reference load cycles  $\bar{N}$ :  $N_e = \bar{N} = 2 \cdot 10^6$   
 B: Slope of the S-N curve k respectively k  
 #: Not possible under overloads because of extreme yielding of the welded low strength joints.

**Tab. 5** Fatigue data

The tests under variable amplitude loading were carried out with a base Gaussian spectrum and a base Gaussian spectrum superimposed with Gaussian distributed overloads, **Fig. 3**, where the maximum overload was higher than the maximum of the base Gaussian spectrum by a factor of 1.4. Also in the case of superimposed loading, the results are presented only in terms of the maximum stress of the base spectrum; the influence of the overloads is included in the fatigue life. In the case of the Gaussian spectrum with overloads, it was not possible to carry out fatigue tests under pulsating loading with the lower-strength steels S355N and S355M because the overloads caused

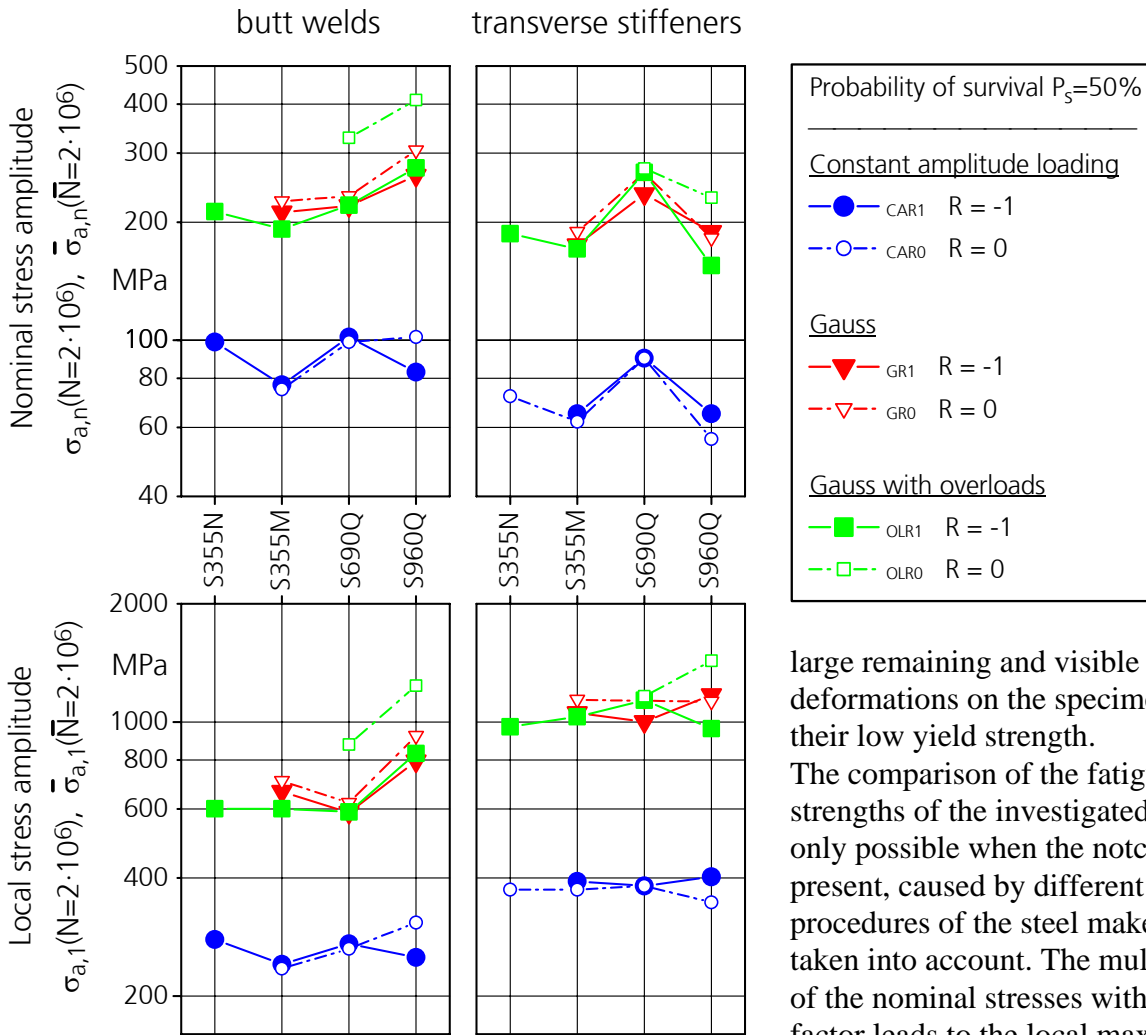


**Fig. 6** Nominal and local stresses

large remaining and visible deformations on the specimens due to their low yield strength.

The comparison of the fatigue strengths of the investigated steels is only possible when the notch factors present, caused by different welding procedures of the steel makers, are taken into account. The multiplication of the nominal stresses with the notch factor leads to the local maximum principal stresses  $\sigma_{a,1}$  ( $P_s = 50\%$ ). In calculating the local stresses the

highest notch factor (probability of occurrence of 10 %) was used, **Tab. 3**. To verify that this value (or a higher one) was responsible for crack initiation, at the location of crack initiation of four butt welded specimens, the geometry was measured after the failure and the notch factor was recalculated; the results demonstrate the fit of the assumption, **Tab. 4**. **Fig. 6** compares the results in the nominal and the local stress systems. Under constant amplitude loading for the four steels, no significant difference in the bearable local stresses for the butt welds can be detected. The results under variable amplitude loading are also compared in **Fig. 6** (local maximum stress amplitude). Once more, the differences between the steels are reduced if the local stresses are compared, where the influence of different weld geometries is eliminated by allowing for the notch factors present. For the butt welds (lower notch factor), advantages for the high-strength steel S960Q (in the case of the normal Gaussian spectrum and in the case of overloads) can be noticed, especially under pulsating loading. For the transverse stiffeners (high notch factor), slight advantages for the high-strength steel S960Q exist, only in the case of pulsating overloads.

Although, for the variable amplitudes, the calculated local stresses (linear elastic material behaviour assumed) are fictitious, because of the limits of yield strengths and the heights of the local peaks, the observed tendencies are genuine.

## 5. EXCEEDANCE OF CONSTANT AMPLITUDE FATIGUE STRENGTH BY VARIABLE AMPLITUDE LOADING AND BENEFITS DUE TO OVERLOADS

In **Fig. 7**, the endurable stresses from the S-N curve and fatigue life curves (Gaussian spectrum without or with overloads) are compared at  $2 \cdot 10^6$  load cycles. The ratio between constant and

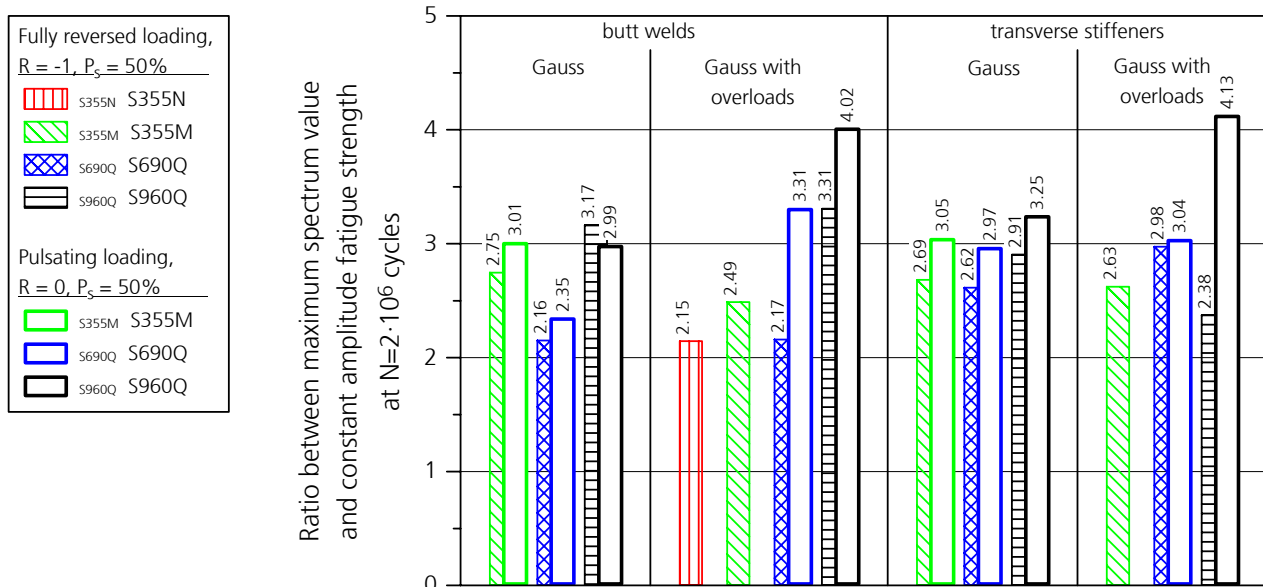


**Fig. 7** Exceedance of constant amplitude fatigue strength by variable amplitude loading

variable amplitude loading, for the different steels, also depends on the particular fatigue strength under constant amplitude loading. So, in addition to the calculated ratio between the two values, the absolute values have also to be taken into account. For example: although high ratios can be found, the bearable amplitudes under constant and variable amplitude loading can be lower than for low ratios.

Exceeding of the constant amplitude fatigue strength by factors between 2.6 and 3.3 is possible in the case of the Gaussian spectrum without overloads, independent of the stress ratio. In the case of the butt welded S690Q only, the factors are about 20 % lower. With regard to the Gaussian spectrum with overloads, factors between 2.2 and 3.3 can be observed. Specifically under pulsating loading, the steel S960Q reaches factors higher than 4.

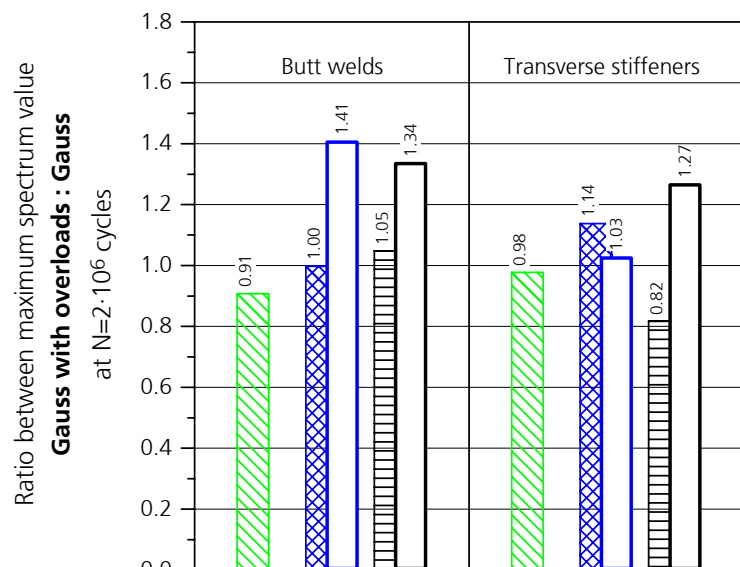


**Fig. 8** Benefits due to overloads (Caption comparable to Fig. 7)

Specifically under pulsating loading, the steel S960Q reaches factors higher than 4.

Comparing the bearable amplitudes at  $\bar{N} = 2 \cdot 10^6$  cycles for the welded joints, no disadvantages in fatigue life due to the selected overloads are detectable in most cases, **Fig. 8**. The fatigue strength decreases only for the S355M (butt weld) and the S960Q (transverse stiffener), in both cases under fully reversed loading.

## 6. INFLUENCE OF MEAN STRESSES IN THE HCF RANGE

Under constant amplitude loading, no or only a slight influence on the fatigue strength can be noticed. In the case of variable amplitude loading, the bearable stress amplitudes under pulsating loading are mostly higher than under fully reversed loading. This observation can only be explained by an assumed long crack propagation phase before failure, where high upper loads ( $\bar{\sigma}_u(R=0) = 2 \cdot \bar{\sigma}_a$ ) lead to a yielding at the crack front. This causes compressive residual stresses, deceleration of crack propagation and the increase of fatigue strength.

## 7. LCF BEHAVIOUR

In the low cycle fatigue range, fatigue tests with transverse stiffeners were carried out and compared as local stress amplitudes versus cycles to rupture. Under fully reversed as well as under pulsating loading, advantages for the high-strength steel S960Q are noticed while the results for S355N, S355M and S690Q can be gathered in one common scatter band. S960Q reaches about a five times higher fatigue life.

## 8. STRAIN CONTROLLED FATIGUE TESTS

Under strain controlled fatigue testing with unnotched specimens in the range of low cycle fatigue, the S960Q (base material and weld metal) reaches higher cycles than the lower grades. The cyclic yield strengths of the weld metals are higher than those of the base materials, except for the steel S960Q, where the two values are approximately equal. In relation to the monotonic yield strength of the base material the cyclic values are lower than the monotonic ones for all steels. In the case of the fatigue strength in the HCF area, derived from the stress controlled fatigue tests with unnotched specimens, up to a cyclic yield strength of 600 MPa (i.e. up to S690Q) the endurance limits for the base material and the weld metal increase; beyond this value, they then remain almost constant (S960Q).

## 9. CRACK INITIATION

With the transverse stiffeners under pulsating loading, the cracks were detected for the four steel grades. S690Q and S960Q have the same slope of the crack initiation curve, which is only slightly flatter than the S-N curve for rupture. In the case of the steels S355N and S355M, it is distinctly more flat. While S690Q has a short phase of crack propagation, this phase is very long for the S960Q; this is related to the respective fatigue strength, which is for the S690Q obviously higher in the nominal stress system. In all cases, the crack started at the weld toe and moved through the heat affected zone.

## 10. FRACTURE MECHANICAL TESTS

For the base material, no significant differences between the steels exist [11, 12]. While for the steels S355N and S355M no difference between base and weld metal can be noticed, the weld metal of the S690Q shows a better crack propagation behaviour than the low grade steels, after deceleration effects in the heat affected zone.

The weld metal of the steel S960Q has a much higher threshold value  $\Delta K_{th}$  than the low-strength steels and also a better crack propagation behaviour in the heat affected zone (HAZ), where the cracks started and propagated through. This is the reason for the slow crack propagation after crack initiation for this steel.

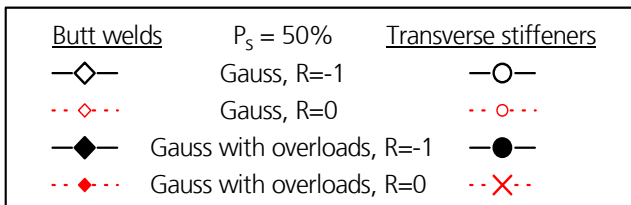
## 11. RESIDUAL STRESS MEASUREMENTS

The levels of residual longitudinal stresses at the transition from the weld metal to the base material of the butt welded specimens and transverse stiffeners have been measured. The hole drilling method has been used for these measurements, in particular the strain gauges have been placed about 5 mm from weld toe and equivalent stresses were derived. The values varied between -383 MPa (compressive stresses) and +187 MPa (tensile stresses). The different values of longitudinal residual stresses were not in agreement with the fatigue behaviour.

## 12. FATIGUE LIFE CALCULATION AND REAL DAMAGE SUMS

One difficulty encountered when estimating fatigue life concerns the assumption of the relevant damage hypothesis and the real damage sum:

$$D = \sum (n/N)_i \leq D_{real} \quad (2)$$



The real damage sums obtained for different fatigue life calculation methods

$$D_{real} = \bar{N}_{r,exp} / \bar{N}_{r,calc} \quad (3)$$

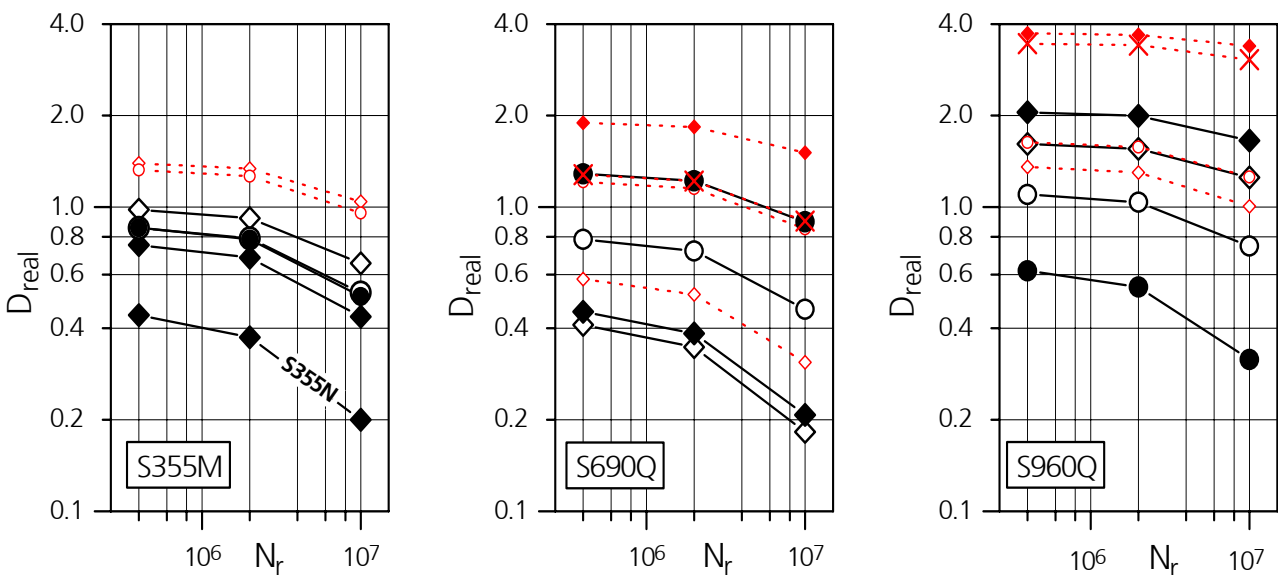


Fig. 9 Real damage sums for welded specimens

are determined here with the linear damage accumulation hypothesis of Palmgren-Miner [13, 14] with a modification of the S-N curve after the knee point proposed by Haibach [15]. The decrease in fatigue strength with propagating damage of the present material is taken into account by means of an extension of the S-N curve beyond the knee point with an inclination of  $k' = 2k - 1$  for steels. A calculation with the original or elementary Miner hypothesis would merely lead to modified real damage sums. The damage calculation presumes that the location of failure under constant amplitude loading must be identical to that for other types of loading. Experience [16] shows a large scatter of the real damage sum; the average value is  $D_{\text{real}} = 0.45$ .

The calculations were carried out for stress levels which lead, under variable amplitude loading, to fatigue lives of  $N_f = 4 \cdot 10^5$ ,  $2 \cdot 10^6$  and  $10^7$  cycles. **Fig. 9** presents the real damage sums for the welded specimens. The following assessments can be made:

- The higher the stress level on which the calculation is carried out, the higher is the real damage sum. The higher the damage sum, the lower is its increase at higher stress levels.
- For the S355M steel, the damage sum varies between  $D_{\text{real}} = 0.4$  and 1.5 (in the one calculated variant of the S355N steel its damage sum was lower than S355M by a factor of 2.), for the S690Q between  $D_{\text{real}} = 0.2$  and 2.0 and for the S960Q between  $D_{\text{real}} = 0.3$  and 4.0
- The averages of the damage sums under pulsating loading ( $R = 0$ ) are higher than those under fully reversed loading ( $R = -1$ ).
- However, the average value of  $D_{\text{al}} = 0.5$  covers most results [17, 18].

### 13. CONCLUSIONS

This investigation was carried out with a view to pointing out the advantages of high-strength steels S690Q and S960Q in the welded state under cyclic constant and variable amplitude loading. The results expected would lead to an increasing use of high-strength steels and support the design of light weight constructions.

The results of the investigation in fact showed, that there is, a priori, no clear advantage for the investigated states of the high-strength steels, butt welds and transverse stiffeners, under constant amplitude loading. In tests with unnotched specimens, removed from the welds (these specimens can be designated as being free from residual stresses), high fatigue strengths have been derived for the weld metal under constant amplitude loading. Under fully reversed loading, about 30 % higher fatigue strengths were reached compared with the low strength steels. This means that the transformation of these results into practice requires the machining of welds, in order to achieve low notch factors and to use the advantages of high-strength steels.

In the case of variable amplitude loading, for the butt welds and transverse stiffeners a large part of fatigue life is associated with crack propagation. The higher the amplitude, the higher are the residual compressive stresses at the crack front, caused by plastic deformation. In this investigation this phenomenon could be put into practice by the S960Q steel in the most effective way: because of its highest yield strength, this material was able to build up the highest compressive residual stresses. Therefore, this material's butt welds endure 30 % higher local stresses than those in the lower grades. Under pulsating loading when overloads occur, a comparison is not possible because of extreme yielding of the welded low strength joints. Stochastically occurring overloads (factor 1.4) in the main do not negatively influence the fatigue life of the investigated steel grades. For the fatigue life assessment, the permissible value  $D_{\text{al}} = 0.5$  can be recommended.

The interaction of a range of different parameters determines the fatigue strength of welded joints: loading, geometry, material and manufacturing. For an optimum design, this interaction must be taken into account and the present results deliver the necessary base for the use of the investigated materials. Further, the investigated weld design classes are in accordance with the Eurocode 3.

## REFERENCES

- [1] ASME Boiler and Pressure Vessel Code, American Society of Mechanical Engineers, New York (1984)
- [2] AD-Merkblatt S 2, Beuth-Verlag, Berlin/Köln (1982)
- [3] British Standard BS 5400, British Standards Institution, London (1980)
- [4] EUROCODE Nr. 3, Stahlbau-Verlagsgesellschaft mbH, Köln (1984)
- [5] Lessels, J., Rohde, W., Pontremoli, M., Devillers, L., ECSC-Contract No. 7210/ZZ/466 (1992)
- [6] ISO/DIS 5817 (Norm-Entwurf), Beuth Verlag, Berlin, Ausgabe 2000-02
- [7] ISO 5817, Beuth Verlag, Berlin, Ausgabe 1992-06
- [8] Anthes, R.J., Köttgen, V.B., Seeger, T., Schweißen und Schneiden 45 (1993), Heft 12, S. 685 – 688
- [9] Haibach, E., Matschke, C., Fraunhofer-Institut für Betriebsfestigkeit LBF, Darmstadt, Bericht Nr. FB-155 (1980)
- [10] Haibach, E., Matschke, C., ASTM STP 770 (1982), p. 549 – 571
- [11] de Back, J., Vaessen, G.H., ECSC - Final Report (7210-KB 16/602), Foundation for Materials Research in Sea, Delft (1988)
- [12] Scholte, H.-G., Wildschut, H., EGKS EUR 7347 (1981), Paper 5.2, p. 1 – 17
- [13] Miner, M.A., Journal of Applied Mechanics 12 (1945) Nr. 3, p. A159 - A164
- [14] Palmgren, A., VDI-Z. 68 (1924) Nr. 14, S. 339 – 341
- [15] Haibach, E., Fraunhofer-Institut für Betriebsfestigkeit LBF, Darmstadt, Technische Mitteilungen Nr. 50/70 (1970)
- [16] Eulitz, K.G., Doecke, H., Esderts, A., Forschungskuratorium Maschinenbau (FKM), Vorhaben Nr. 152, Forschungsheft 189 (1994).
- [17] Lagoda, T., Sonsino, C.M., Materialwissenschaft und Werkstofftechnik 35 (2004), Heft 1, S. 13 – 20
- [18] Sonsino, C.M., Maddox, S.J., Hobbacher, A., Proceedings of the IIW International Conference on Technical Trends and Future Perspectives of Welding Technology for Transportation, Land, Sea, Air and Space (2004), p. 84-99